

Journal Pre-proofs

Research paper

Functionalized calcium carbonate (FCC) as a novel carrier to solidify supersaturated self-nanoemulsifying drug delivery systems (super-SNEDDS)

Jumana Merchant, Anette Müllertz, Thomas Rades, Jacob Bannow

PII: S0939-6411(23)00290-4
DOI: <https://doi.org/10.1016/j.ejpb.2023.11.001>
Reference: EJPB 14136

To appear in: *European Journal of Pharmaceutics and Biopharmaceutics*

Received Date: 8 August 2023
Revised Date: 27 October 2023
Accepted Date: 2 November 2023

Please cite this article as: J. Merchant, A. Müllertz, T. Rades, J. Bannow, Functionalized calcium carbonate (FCC) as a novel carrier to solidify supersaturated self-nanoemulsifying drug delivery systems (super-SNEDDS), *European Journal of Pharmaceutics and Biopharmaceutics* (2023), doi: <https://doi.org/10.1016/j.ejpb.2023.11.001>

This is a PDF file of an article that has undergone enhancements after acceptance, such as the addition of a cover page and metadata, and formatting for readability, but it is not yet the definitive version of record. This version will undergo additional copyediting, typesetting and review before it is published in its final form, but we are providing this version to give early visibility of the article. Please note that, during the production process, errors may be discovered which could affect the content, and all legal disclaimers that apply to the journal pertain.

© 2023 Published by Elsevier B.V.



1 **Functionalized calcium carbonate (FCC) as a novel carrier to** 2 **solidify supersaturated self-nanoemulsifying drug delivery systems** 3 **(super-SNEDDS)**

4 Jumana Merchant¹, Anette Müllertz¹, Thomas Rades¹, Jacob Bannow¹

5 ¹*Department of Pharmacy, University of Copenhagen, Copenhagen, Denmark*

6

7 **Abstract**

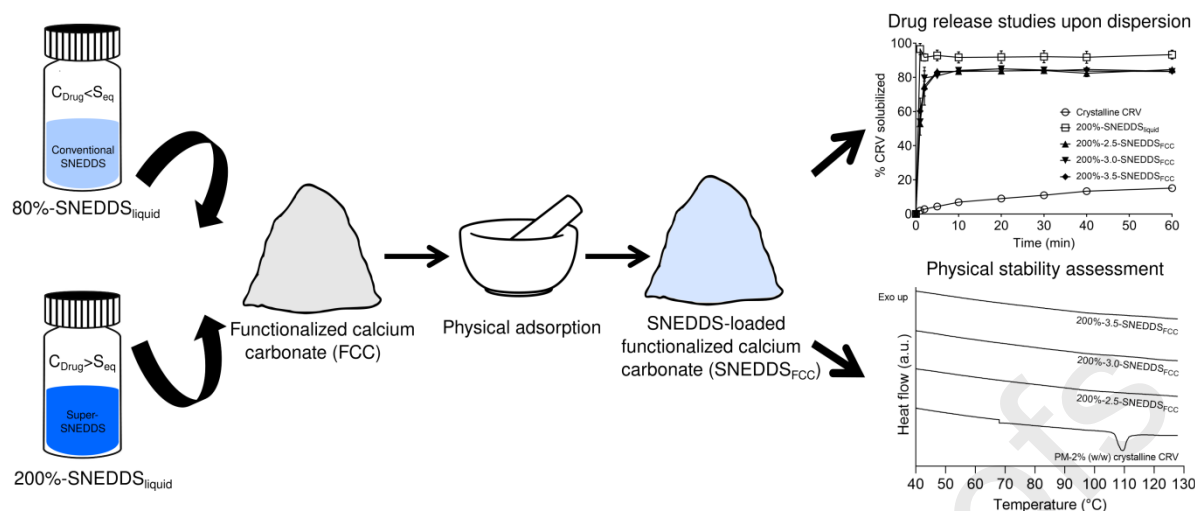
8 Functionalized calcium carbonate (FCC), a novel pharmaceutical excipient, has shown promising
9 properties in the field of oral drug delivery. The current study aimed at evaluating the feasibility of FCC
10 as a carrier for the solidification of self-nanoemulsifying drug delivery systems (SNEDDS) containing
11 the poorly water-soluble model drug carvedilol (CRV). Conventional, subsaturated SNEDDS (80%-
12 SNEDDS_{liquid}) and supersaturated SNEDDS (200%-SNEDDS_{liquid}) were loaded onto FCC via physical
13 adsorption at three ratios; 2.5:1, 3.0:1 and 3.5:1 (w/w) of FCC:SNEDDS_{liquid}, respectively, generating
14 free-flowing powders (SNEDDS_{FCC}) with drug loading ranging from 0.8% to 2.6% (w/w) CRV. The
15 emulsification of SNEDDS_{FCC} in a USP II dissolution setup (in purified water) was characterized using
16 dynamic light scattering, resulting in similar droplet sizes and PDIs as observed for their liquid
17 counterparts. The morphology and physical state of the obtained SNEDDS_{FCC} were characterized using
18 scanning electron microscopy and differential scanning calorimetry. The physical stability and drug
19 release upon dispersion were assessed as a function of storage time. The 200%-SNEDDS_{liquid} were
20 physically stable for 6 days, however, solidification using FCC stabilized the supersaturated
21 concentrations of CRV for a test period of up to 10 weeks (solidification ratios 3.0:1 and 3.5:1
22 (FCC:SNEDDS_{liquid})). SNEDDS_{FCC} achieved an improved rate and extent of drug release upon
23 dispersion compared to the crystalline CRV in tap water (pH 7.5), however, to a lesser extent than their
24 liquid counterparts. After 8 weeks of storage (25 °C at dry conditions), FCC was still able to rapidly
25 release the SNEDDS_{liquid} and demonstrated the same rate and extent of drug release as freshly prepared
26 samples. The solidification of 200%-SNEDDS_{liquid} in presence of FCC greatly improved the drug
27 loading and showed an enhanced drug release profile compared to the conventional systems. In
28 conclusion, FCC showed potential as a carrier for solidification of SNEDDS and for the development
29 of novel supersaturated solid SNEDDS for the oral delivery of poorly water-soluble drugs.

30 **Keywords**

31 Oral drug delivery, Lipid-based drug delivery, Self-nanoemulsifying drug delivery systems,
32 Functionalized calcium carbonate, Solidified lipid-based systems, Carvedilol, Solid-state analysis

33 **Graphical Abstract**

34



35

36 Introduction

37 Oral drug delivery is the most favored route of drug administration due to its potential advantages
 38 including patient compliance, cost-effectiveness and non-invasiveness [1]. In a recent report (2021),
 39 90% of the new drug candidates emerging from the pharmaceutical industry were classified as poorly
 40 water-soluble [2], leading to low and erratic bioavailability from conventional dosage forms after oral
 41 administration [3]. Hence, enabling formulation strategies are needed to improve the bioavailability of
 42 poorly water-soluble drugs after oral administration [4].

43 Lipid-based formulations (LBF) offer a solution by mitigating the inherently slow dissolution process
 44 of poorly water-soluble drugs due to their ability to pre-dissolve lipophilic drugs and thus circumvent
 45 the dissolution step in the gastrointestinal tract [5–7]. Amongst the various LBF, the use of a self-
 46 nanoemulsifying drug delivery system (SNEDDS) has attracted significant attention [8]. SNEDDS
 47 consists of drugs dissolved in an isotropic mixture of lipids, surfactants, co-surfactants and co-solvents
 48 from which a nanoemulsion is formed upon dispersion in aqueous media [7]. Conventional SNEDDS
 49 usually have a drug load between 50% to 90% of the drug's equilibrium solubility (S_{eq}) in the SNEDDS
 50 preconcentrate to avoid drug precipitation during storage and after administration [9]. The low drug
 51 loading of conventional SNEDDS potentially results in the administration of several dosage units,
 52 negatively affecting patient compliance [10]. To increase the drug loading in SNEDDS preconcentrate,
 53 Thomas et al. [9,11] developed the concept of supersaturated SNEDDS (super-SNEDDS). Super-
 54 SNEDDS are characterized by containing drug concentrations well beyond the drug's S_{eq} in the
 55 SNEDDS preconcentrate and have been demonstrated to be suitable alternatives to conventional
 56 SNEDDS [9,11,12].

57 Despite the mentioned advantages, some limitations still exist for SNEDDS. They are usually filled in
 58 soft gelatin capsules, therefore limiting the drug loading by the fill weight and the drug solubility in the
 59 formulation [13,14]. Furthermore, nearly all development and manufacturing activities involving soft
 60 gelatin capsules are outsourced to contract manufacturing organizations since most pharmaceutical
 61 companies lack in house capability leading to high production costs [15]. In an attempt to overcome
 62 these limitations, the solidification of liquid SNEDDS using chemically inert solid carriers to enable
 63 the production of solid dosage forms has attracted substantial interest in recent years [16].

64 The general hypothesis applied is that the development of solidified SNEDDS could combine the
 65 advantages of liquid SNEDDS with the high physical stability of solid dosage forms while enhancing
 66 or retaining the biopharmaceutical performance of the poorly water-soluble drugs compared to their
 67 liquid counterparts [17]. Moreover, the ease of manufacturing associated with low costs and the
 68 possibility of producing a wider range of dosage forms, e.g., powder filled in sachets or capsules or
 69 compressed into tablets, makes solidification attractive from an industrial perspective [16,18,19].

70 A plethora of research is devoted to the transformation of liquid LBF into solid dosage forms with a
71 focus on various solidification methods as well as on the selection of solid carrier excipients. The
72 solidification methods most commonly employed are physical adsorption, spray drying and melt
73 extrusion [18]. A wide range of inorganic porous carriers for the solidification of LBF has been
74 investigated including magnesium aluminometasilicate (e.g. Neusilin®), colloidal silicon dioxide (e.g.
75 Aerosil®), porous amorphous silica gels (e.g. Sylysia® and Syloid®), and calcium silicate (e.g.
76 Hubersorb®) [20]. An appropriate selection of the solid carrier for the solidification of LBF should
77 enable the highest possible lipid (and drug) loading efficiency, adequate flowability, compactability, as
78 well as an efficient re-dispersibility after administration [21,22].

79 In order for the loaded poorly water-soluble drug to be released from the solid carrier, the liquid lipid
80 phase of the solid dosage form has to desorb from the solid carrier and partition into the aqueous phase,
81 or the solid carrier itself has to dissolve within the gastrointestinal tract [16]. Over the past years, various
82 solid carriers have been investigated with respect to their role in retaining or enhancing the
83 biopharmaceutical performance of solidified LBF. However, conflicting evidence has been reported as
84 to whether the solidified formulations will preserve, enhance, or decrease the biopharmaceutical
85 performance compared to their respective liquid counterparts. While several studies reported complete
86 drug release from the solidified LBF [23–26], others observed incomplete desorption from solidified
87 formulations translating to a reduced *in vivo* performance [14,27–29].

88 Neusilin®, a mesoporous magnesium aluminometasilicate, demonstrated significant potential as a solid
89 carrier for LBF due to its ability to generate solidified LBF by simple physical adsorption and direct
90 compactability allowing the manufacturing of tablets [30]. However, the suitability of Neusilin® as a
91 solid carrier for LBF has been discussed controversially. Incomplete drug release was identified to be a
92 major issue with formulations containing Neusilin® as a solid carrier due to the formation of gels by
93 lipid-surfactants mixtures once in contact with water, hindering the drug release from deeper pores of
94 Neusilin® [14,15,30]. A further reduction of drug release from the solidified LBF upon storage has
95 been a concern, possibly due to the progressing migration of the mobile fractions of liquid LBF to
96 deeper unwetted regions of the carrier during storage, entrapping the drug deeper within the pores [20].

97 The above-mentioned limitations drive the need to investigate the potential of new solid carriers for the
98 solidification of LBF. In a previous study, solid supersaturatable SNEDDS loaded with glipizide were
99 developed using conventional calcium carbonate, in combination with talc and hydroxypropyl
100 methylcellulose (HPMC-E5) as polymeric precipitation inhibitor (PPI). However, the primary objective
101 of the study was to evaluate the potential of HPMC-E5 in stabilizing the resulting supersaturated drug
102 concentrations following dispersion [31].

103 Functionalized calcium carbonate (FCC) was recently identified as a novel pharmaceutical excipient
104 for the oral delivery of poorly water-soluble drugs [32]. FCC is a microparticulate material ranging
105 from 5-15 µm in diameter [33]. The small pore diameter (0.01-1 µm) and thus resulting high specific
106 area of FCC enables water absorption at a faster rate and 10 times higher extent than conventional
107 calcium carbonate [32,34]. The physical attributes of FCC led to the exploration of this material in the
108 field of pharmaceutical excipient research, resulting in the development of several innovative drug
109 delivery systems. FCC has been investigated as mucoadhesive delivery systems for colon targeting [35],
110 oral protein delivery systems [36], orally dispersible tablets [34,37], floating tablets [38] and as a carrier
111 for increasing the physical stability of amorphous drugs [39].

112 Since FCC has not been studied as a pharmaceutical excipient for the solidification of SNEDDS, the
113 overall objective of this study was to investigate the feasibility of FCC to serve as a solid carrier for
114 conventional SNEDDS and super-SNEDDS. It was hypothesized that the adsorption of super-SNEDDS
115 onto FCC would increase the physical stability of the utilized BSC II model drug carvedilol (CRV) and
116 help to achieve a greater CRV load. The developed solid (super-)SNEDDS and their liquid counterparts
117 were characterized with respect to their *in vitro* performance including droplet size measurements and
118 drug release upon dispersion. The developed solid (super-)SNEDDS were further characterized for drug
119 release upon dispersion as a function of storage time.

120 **Materials and Methods**121 *Materials*

122 Functionalized calcium carbonate (FCC) (Omyapharm® 500 – OG) was obtained from Omya
123 International AG (Oftringen, Switzerland). Carvedilol (CRV) was purchased from Cipla Ltd. (Mumbai,
124 India). Capmul MCM C8 EP/NF (medium chain (MC) mixed glycerides) and Captex 300 EP/NF (MC
125 triglycerides) from Abitec (Columbus, OH, USA) were provided by Barentz (Odense, Denmark).
126 Kolliphor RH40 (polyoxyl 40 hydrogenated castor oil) was donated by BASF (Ludwigshafen,
127 Germany). Transcutol was donated by Gattefossé (Saint Priest, France). Potassium phosphate
128 monobasic and potassium chloride were purchased from Sigma Aldrich (St Louis, MO, USA).
129 Hydrochloric acid 37% (HCl) and acetonitrile (HPLC grade) were purchased from VWR Chemicals
130 (Herlev, Denmark). Purified water was obtained from a SG Ultraclear water system (SG Water GmbH,
131 Barsbüttel, Germany). Tap water (pH 7.5) was used through the course of the study.

132 *Methods*133 *Preparation of liquid SNEDDS (SNEDDS_{liquid})*

134 The MC mixed glycerides (Capmul MCM C8 EP/NF) and the surfactant (Kolliphor RH40) were molten
135 at approximately 50 °C before they were blended in a vortex mixer with the MC triglycerides (Captex
136 300 EP/NF). After equilibration to room temperature, the co-solvent (Transcutol) was added to the
137 mixture followed by a second mixing step forming an isotropic mixture consisting of 51% (w/w) lipid
138 (18% (w/w) Capmul MCM C8 EP/NF and 33% (w/w) Captex 300 EP/NF), 43% (w/w) surfactant
139 (Kolliphor RH40) and 6% (w/w) co-solvent (Transcutol). The generated blank-SNEDDS_{liquid} (drug-
140 free) were subsequently left for overnight stirring at 37 °C and were stored at 25 °C until use.

141 The S_{eq} of CRV in the blank-SNEDDS_{liquid} was determined at room temperature using a shake flask
142 method adapted from Thomas et al. (2012) [9]. Samples were withdrawn at regular intervals and S_{eq}
143 was assumed to have been achieved when consecutive solubility values differed by less than 5%,
144 resulting in an S_{eq} of 47 ± 0.5 mg/g. Conventional SNEDDS (80%-SNEDDS_{liquid}) and super-SNEDDS
145 (200%-SNEDDS_{liquid}) were produced using a heating-cooling cycle at levels corresponding to 80% and
146 200% of the drugs S_{eq} , respectively. Based on the drug load, the required amounts of CRV and blank-
147 SNEDDS_{liquid} were accurately weighed into dust-free glass vials containing a magnetic stirring bar. The
148 mixtures were vortexed at room temperature for 30 s and subsequently ultrasonicated for 15 min at
149 room temperature in a Branson 5510 ultrasonic bath (Branson Ultrasonics, Danbury, CT, USA). To
150 facilitate complete dissolution of the drug, the obtained suspensions were placed in a silicon oil bath
151 (60 °C) and stirred for 1 h (Arex Digital PRO, Heating Magnetic stirrer, VELP® Scientifica, Usmate
152 (MB), Italy). After the heating cycle, the prepared formulations were allowed to slowly equilibrate to
153 25 °C inside the oil bath resulting in isotropic 80%-SNEDDS_{liquid} and 200%-SNEDDS_{liquid}. The
154 magnetic stirring bar was removed, and the vials were stored at 25 °C. The complete dissolution of the
155 CRV after the heating-cooling cycle in all formulations was assessed using polarized light microscopy
156 (PLM) (see below). After the heating-cooling cycle, the chemical stability of CRV in 200%-
157 SNEDDS_{liquid} was determined and an average of $99.7 \pm 3.3\%$ of the added CRV content was detected,
158 indicating chemical stability of CRV during the drug loading procedure. Samples were stored in sealed
159 glass vials at 25 °C and produced in triplicates to assess their physical stability. The vials were analyzed
160 at regular intervals for possible precipitation of the dissolved drug by both visual observation and PLM
161 (see below).

162 *Adsorption of SNEDDS_{liquid} onto FCC (SNEDDS_{FCC})*

163 Adsorption of SNEDDS_{liquid} onto FCC was achieved by manual mixing using a mortar and pestle. First,
164 FCC and SNEDDS_{liquid} were mixed at a ratio of 1:1 (expressed as the weight ratio of
165 FCC:SNEDDS_{liquid}). The amount of FCC was gradually increased until a free-flowing powder was
166 obtained. The following ratios of FCC:SNEDDS_{liquid} were evaluated: 2.5:1, 3.0:1, 3.5:1 (w/w). The

167 resulting mixtures were gently mixed in a mortar for 3 min to obtain a free-flowing powder. The
168 efficiency of the loading procedure was evaluated based on visual inspection of the powder's
169 appearance and flowability. Accordingly, 100 mg of SNEDDS_{liquid} (corresponding to 3.76 mg CRV for
170 80%-SNEDDS_{liquid} and 9.4 mg CRV for 200%-SNEDDS_{liquid}) were loaded onto 250 mg, 300 mg and
171 350 mg of FCC. Hence, six SNEDDS_{FCC} were produced as follows: (A) 80%-2.5-SNEDDS_{FCC}; (B)
172 80%-3.0-SNEDDS_{FCC}; (C) 80%-3.5-SNEDDS_{FCC}; (D) 200%-2.5-SNEDDS_{FCC}; (E)
173 200%-3.0-SNEDDS_{FCC}; (F) 200%-3.5-SNEDDS_{FCC} with CRV loading ranging from 0.8% to 2.6%
174 (w/w).

175 *Drug loading efficiency*

176 The CRV loading efficiency after adsorption of SNEDDS_{liquid} onto FCC was assessed by HPLC. Powder
177 samples of 80%-SNEDDS_{FCC} and 200%-SNEDDS_{FCC} were collected from three different parts of the
178 powder, placed in volumetric flasks and suspended in a mixture of phosphate buffer (0.02M, pH 2) and
179 acetonitrile (55:45% (v/v)). The samples were subsequently ultrasonicated for 20 min in a Branson 5510
180 ultrasonic bath (Branson Ultrasonics, Danbury, CT, USA). The obtained SNEDDS_{FCC} suspensions were
181 centrifuged for 15 min at 13,300 rpm (17,000g) (MicroCL 17 Centrifuge, Thermo Scientific, Waltham,
182 MA, USA) followed by HPLC quantification of the CRV concentration in the clear supernatant. Each
183 formulation was prepared in triplicates and sampling was done from three parts of the SNEDDS_{FCC}
184 powder; thus, the total number of measurements was n=9. The CRV contents are represented as
185 quantified mass of CRV (mg) obtained from HPLC analysis compared to the theoretical mass of CRV
186 (mg).

187 *Solid-state characterization*

188 The surface morphology of neat CRV, neat FCC and SNEDDS_{FCC} (80% and 200%) was studied by
189 scanning electron microscopy (SEM) using a Hitachi TM3030 tabletop microscope (Hitachi High
190 Technologies Europe GmbH, Krefeld, Germany) operated at an accelerating voltage of 15 kV. Samples
191 were sputter coated with gold (Cressington 108 auto, Cressington Scientific Instruments, Watford, UK)
192 prior to SEM analysis.

193 X-ray powder diffraction (XRPD) measurements were performed for neat CRV, neat FCC, physical
194 mixtures, and SNEDDS_{FCC} (80% and 200%) using an X'Pert PANalytical PRO X-ray diffractometer
195 (PANalytical, Almelo, The Netherlands). Physical mixtures were prepared by manually mixing CRV
196 and FCC at different drug to excipient weight ratios (2.5%–20% CRV). Cu K α radiation ($\lambda= 1.54187$
197 Å) was generated using a 45 kV acceleration voltage and current of 40 mA. Samples were scanned in
198 reflectance mode from 5–16° 2 θ with a scan rate of 0.016834° 2 θ /s and a step size of 0.0065652° 2 θ .
199 The data was collected and analyzed using the software X'Pert Data Collector (version 2.2.4)
200 (PANalytical, Almelo, The Netherlands).

201 Neat CRV, neat FCC, individual SNEDDS excipients, SNEDDS_{FCC} (80% and 200%) and physical
202 mixtures (PM) were analyzed using differential scanning calorimetry (DSC) using a Discovery DSC
203 (TA Instruments, New Castle, DE, USA). The PM were prepared by mixing 100 mg of blank-
204 SNEDDS_{liquid}, 350 mg FCC and the corresponding amount of CRV. All the SNEDDS_{FCC} were stored in
205 a desiccator under dry conditions over silica gel at 25 °C and checked for potential CRV
206 recrystallization over a period of 10 weeks. Samples were regularly analyzed by DSC (weekly for the
207 first 4 weeks, and every 2 weeks thereafter) until a CRV melting endotherm was detected. All
208 SNEDDS_{FCC} used for the physical stability assessment were produced in triplicates. A sample mass of
209 3-5 mg was transferred to Tzero aluminium pans and sealed with pierced hermetic Tzero lids. All
210 measurements were carried out using a heating rate of 10 °C/min from a starting temperature of 10 °C
211 (isothermal for 2 min) to an end temperature of 130 °C under a nitrogen gas flow of 50 mL/min. The
212 obtained thermograms were analyzed using TRIOS software (TA Instruments, New Castle, DE, USA).

213 *Droplet size measurements*

214 The droplet size after dispersion of the SNEDDS_{FCC} (80% and 200%) and their respective liquid
215 counterparts was measured by dynamic light scattering (DLS) using a Zetasizer Nano (Malvern,
216 Worcestershire, UK) operated at 37 °C. A USP type II dissolution apparatus consisting of a set of mini
217 glass vessels with rotating mini paddles (Erweka DT600 dissolution tester, Erweka GmbH,
218 Heusenstamm, Germany) was used to promote emulsification in two media, i.e. purified water and HCl
219 solution (0.2M, pH 1.6).

220 Approximately 100 mg of SNEDDS_{FCC} (80% and 200%) and their respective SNEDDS_{liquid} were
221 weighed into the vessel and 100 mL of pre-heated purified water or HCl solution (0.2M, pH 1.6) was
222 added. The dispersions were stirred at 100 rpm for 30 min at 37 ± 0.5 °C. After 30 min, 1 mL aliquots
223 were withdrawn from the vessel. For all SNEDDS_{FCC} dispersed in purified water, the turbid dispersions
224 were centrifuged at 13,300 rpm (17,000g) for 15 min. After centrifugation, the particle size in the
225 obtained supernatant was immediately analyzed without further dilution. The droplet sizes of the
226 resulting dispersions from SNEDDS_{FCC} dispersed in HCl solution (0.2M, pH 1.6) and SNEDDS_{liquid}
227 were immediately analyzed from aliquots directly taken from the vessel, without further dilution. In the
228 case of SNEDDS_{FCC} dispersed in HCl solution (0.2M, pH 1.6), no centrifugation step was necessary
229 due to the apparent solubility of FCC in acidic media. Additionally, droplet size measurements for
230 blank-SNEDDS_{liquid}, and blank-SNEDDS_{FCC} were performed as controls. The measured droplet size and
231 PDI of three independent measurements per formulation are reported as mean z-average (nm) and PDI,
232 respectively.

233 *Drug release upon dispersion*

234 Drug release upon dispersion of SNEDDS_{FCC} (80% and 200%), SNEDDS_{liquid} (80% and 200%) and
235 crystalline CRV was quantified in 100 mL of tap water (pH 7.5) using a USP type II apparatus consisting
236 of a set of mini glass vessels with rotating mini paddles (Erweka DT600 dissolution tester, Erweka
237 GmbH, Heusenstamm, Germany) under sink conditions. A sample amount corresponding to 3.76 mg
238 of CRV was used corresponding to a lipid content of 100 mg for 80%-SNEDDS_{FCC} and 40 mg for
239 200%-SNEDDS_{FCC}. The paddle rotation speed was set to 100 rpm and the temperature of the media
240 was maintained at 37 ± 0.5 °C. Aliquots (3 mL) were withdrawn at predetermined time points (1, 2, 5,
241 10, 15, 20, 30, 40 and 60 min) and the volume was replaced by fresh, pre-heated media. The samples
242 were centrifuged at 13,300 rpm (17,000g) for 1 min and the obtained supernatant was diluted
243 appropriately and subsequently analyzed by HPLC (see below). All measurements were carried out in
244 triplicates.

245 The drug release studies were performed for freshly prepared samples (week 0) and after 3, 6 and 8
246 weeks of storage. The samples were stored in a desiccator under dry conditions over silica gel at 25 °C
247 and analyzed for CRV drug release upon dispersion. All the SNEDDS_{FCC} used for the drug release
248 assessment during storage were produced in triplicates.

249 *HPLC analysis*

250 Quantification of CRV in samples obtained from the S_{eq} quantification, solidification efficiency
251 assessment, chemical stability study and drug release studies were performed using an Ultimate 3000
252 Ultraviolet (UV) detector, UltiMate 3000 autosampler and UltiMate 3000 pump (Thermo Scientific,
253 Waltham MA, USA) equipped with an ACE Excel 5 C18AR column (Advanced Chromatography
254 Technologies Ltd., Aberdeen, Scotland). The mobile phase consisted of phosphate buffer (0.02 M, pH
255 2) and acetonitrile (55:45% (v/v)). The injection volume was 20 µL at a flow rate of 1.0 mL/min. The
256 eluted CRV was detected at a wavelength of 240 nm.

257 *Polarized light microscopy*

258 SNEDDS_{liquid} (80% and 200%) were analyzed for undissolved crystalline CRV after the heating and
259 cooling cycle and for precipitation of CRV upon storage using a Leica DM LM microscope equipped
260 with cross polarizers (Leica Microsystems, Wetzlar, Germany). Images were acquired using a Media

261 Cybernetics Evolution MP digital camera and the ImagePro Insight software version 8.0 (Media
262 Cybernetics).

263 *Statistical analysis*

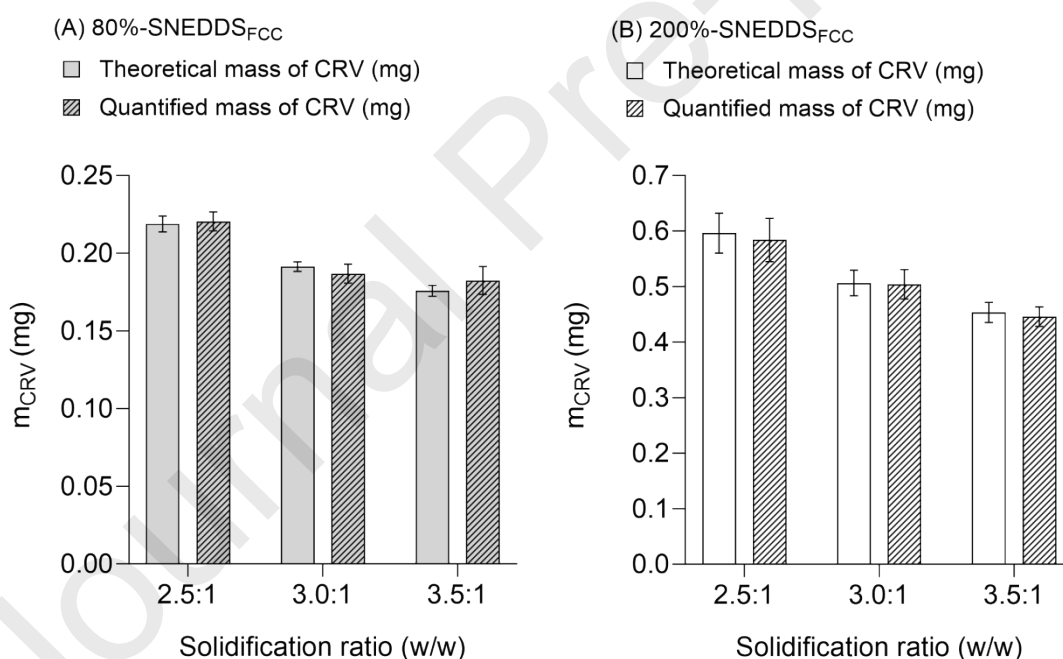
264 Statistical analysis was carried out using GraphPad Prism (Version 9.5.0, GraphPad Software, San
265 Diego, CA, USA). Unpaired Student's t-tests were applied to determine statistically significant
266 differences ($p = 0.05$) between two groups, whereas analysis of variance (ANOVA) followed by
267 Tukey's post-test were utilized for differences between more than two groups ($p = 0.05$).

268

269 **Results and discussion**

270 *Drug loading efficiency*

271 To ensure a uniform drug distribution after the adsorption of SNEDDS_{liquid} onto FCC, the content
272 uniformity of CRV was studied. As shown in Figure 1, for both drug loadings (80%-SNEDDS_{FCC} and
273 200%-SNEDDS_{FCC}) and their corresponding solidification ratios (2.5:1, 3.0:1, and 3.5:1 (w/w)) no
274 statistically significant difference between the theoretical mass of CRV and the corresponding
275 quantified mass of CRV was observed ($p > 0.05$). This indicates that the employed solidification
276 method by manual mixing using a mortar and pestle resulted in a uniform distribution of CRV in
277 SNEDDS_{FCC}.



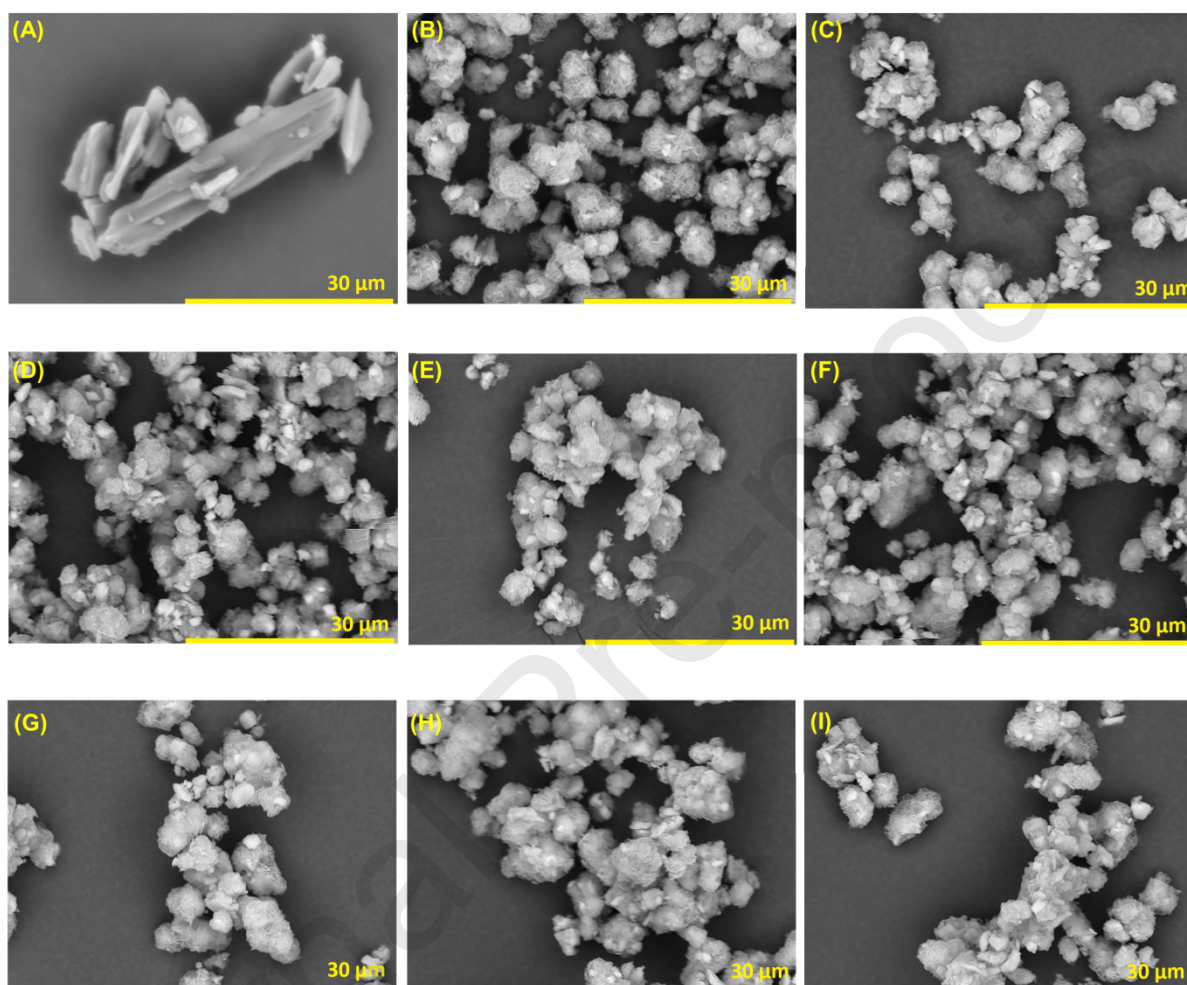
278

279 **Figure 1.** Quantified mass of CRV (*dashed columns*) compared to the theoretical mass of CRV (*solid*
280 *columns*) for (A) 80%-SNEDDS_{FCC} (*light grey columns*) and (B) 200%-SNEDDS_{FCC} (*white columns*)
281 at solidification ratios of 2.5:1, 3.0:1, and 3.5:1 (w/w). Results are represented as mean \pm SD (n=9).

282 *Solid state characterization*

283 SEM analysis of SNEDDS_{FCC} was carried out to study the surface morphology of FCC particles before
284 and after loading with SNEDDS_{liquid}. The morphology of neat CRV, neat FCC, blank-SNEDDS_{FCC} and
285 SNEDDS_{FCC} are shown in the SEM images in Figure 2. Blank-SNEDDS_{liquid} was loaded onto FCC as a
286 reference (blank-SNEDDS_{FCC}, Figure 2 (C)) to study the surface morphology of FCC particles after

287 lipid-loading (drug-free) and enable a comparison with neat FCC particles (Figure 2 (B)). SNEDDS_{FCC}
 288 for both drug loadings and the corresponding solidification ratios (2.5:1, 3.0:1, and 3.5:1 (w/w)) retained
 289 the original shape of the neat FCC particles while showing no signs of CRV crystals (Figure 2 (A)).
 290 The developed SNEDDS_{FCC} formulations appeared no different to the neat FCC and the blank-
 291 SNEDDS_{FCC} particles at CRV loading of 0.8% to 2.6% (w/w), suggesting a complete adsorption of
 292 drug-loaded SNEDDS_{liquid} onto FCC.



293

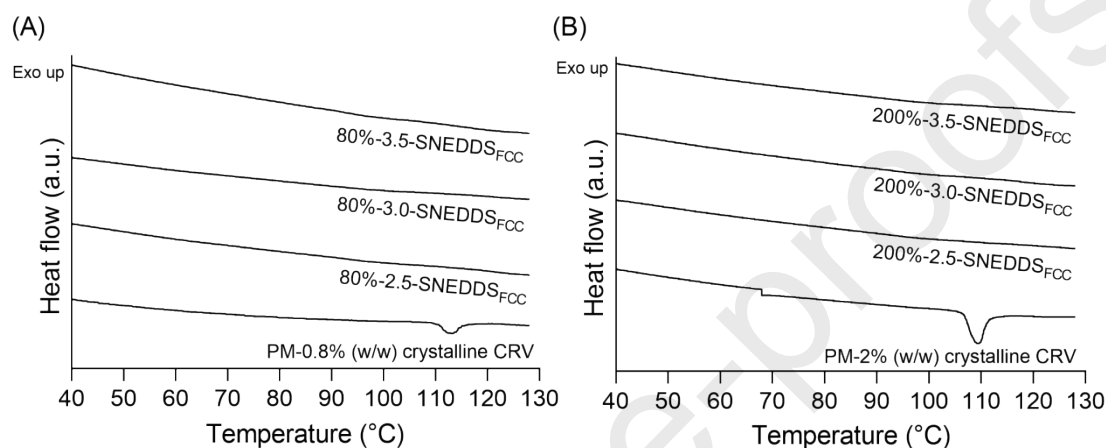
294 **Figure 2.** SEM images of (A) neat CRV; (B) neat FCC; (C) blank-SNEDDS_{FCC}; (D)
 295 80%-2.5-SNEDDS_{FCC}; (E) 80%-3.0-SNEDDS_{FCC}; (F) 80%-3.5-SNEDDS_{FCC}; (G)
 296 200%-2.5-SNEDDS_{FCC}; (H) 200%-3.0-SNEDDS_{FCC}; (I) 200%-3.5-SNEDDS_{FCC} loaded via physical
 297 adsorption. All SEM images were obtained at a magnification of x3000.

298 As the amount of CRV present in the developed SNEDDS_{FCC} ranged from 0.8% to 2.6% (w/w), XRPD
 299 showed an insufficient limit of detection (LOD) to detect potentially recrystallized CRV (see
 300 supplementary information, Figure S1). Thus, the feasibility of using DSC for the detection of low
 301 amounts of crystalline CRV in SNEDDS_{FCC} during the physical stability study was investigated.

302 DSC thermograms of the individual excipients and neat CRV are presented in Figure S2 (supplementary
 303 information). Neat crystalline CRV displayed a sharp melting endotherm with an onset temperature of
 304 115.4 °C, corresponding to its characteristic melting point [40]. PMs ranging from 2%-0.04% (w/w) of
 305 crystalline CRV were analyzed using DSC to determine the LOD for CRV in the FCC matrix
 306 (supplementary information, Figure S3). The PM containing 2%, 0.8%, 0.52%, 0.2%, and 0.08% (w/w)
 307 of crystalline CRV in FCC displayed an endothermic peak corresponding to the melting of crystalline
 308 CRV. However, no melting endotherm was observed for the PM containing 0.04% (w/w) of crystalline

309 CRV. Consequently, the LOD of crystalline CRV using DSC was found to be 0.08% (w/w) CRV,
 310 demonstrating a sufficient sensitivity to detect the recrystallization of 3% of the loaded CRV in
 311 200%-2.5-SNEDDS_{FCC} (or 10% recrystallization of the loaded CRV in the 80%-3.5-SNEDDS_{FCC}).

312 The DSC thermograms of freshly prepared samples of 80%-SNEDDS_{FCC} and 200%-SNEDDS_{FCC} are
 313 shown in Figure 3(A) and Figure 3(B), respectively. The DSC thermograms of 80%-SNEDDS_{FCC} and
 314 200%-SNEDDS_{FCC} displayed no characteristic CRV melting endotherm for freshly prepared samples,
 315 indicating the presence of dissolved CRV in the SNEDDS_{FCC}. The obtained results demonstrate the
 316 ability of FCC to act as a solid carrier maintaining CRV in a dissolved state even at supersaturated
 317 concentrations of CRV in the adsorbed 200%-SNEDDS_{liquid} after the initial loading procedure.



318

319 **Figure 3.** DSC thermograms of freshly prepared samples of (A) 80%-SNEDDS_{FCC} and (B) 200%-
 320 SNEDDS_{FCC} and their corresponding PM containing 0.8% (w/w) and 2% (w/w) crystalline CRV,
 321 respectively. The DSC thermograms shown for the developed SNEDDS_{FCC} are representative results
 322 for one of the triplicate samples.

323 *Physical stability studies*

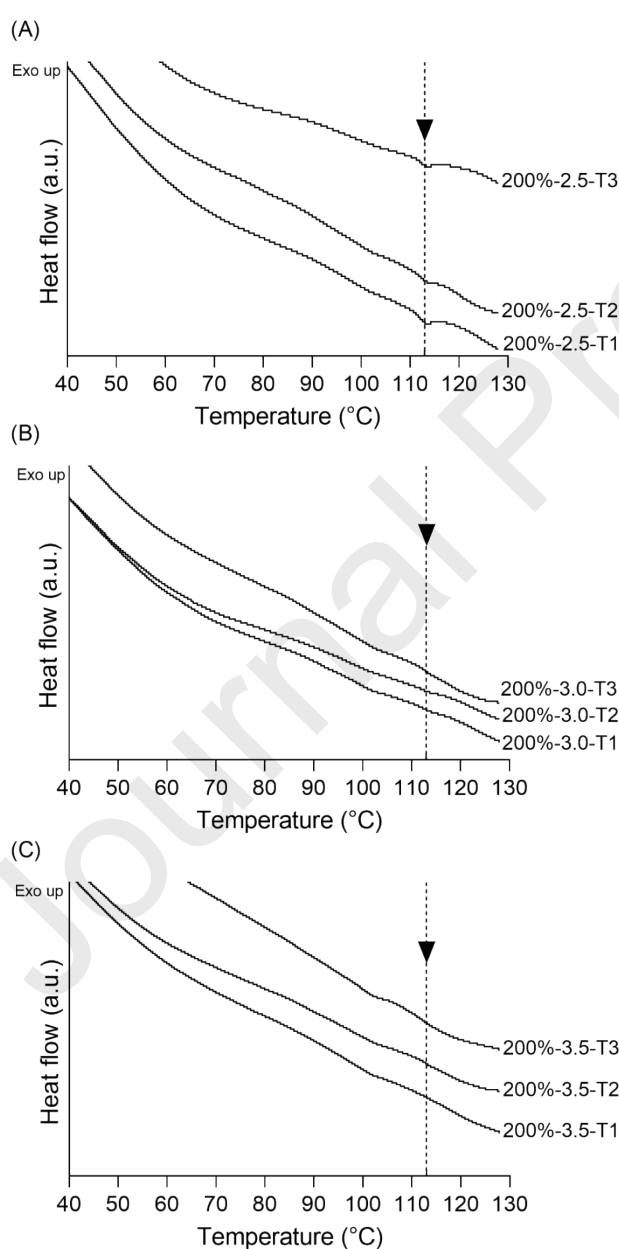
324 The SNEDDS_{liquid} were inspected on a regular basis by PLM, and the onset of CRV precipitation in
 325 SNEDDS_{liquid} was defined as the time point when crystals were detected by PLM in at least one of the
 326 prepared triplicate samples. Since the 80%-SNEDDS_{liquid} contained CRV concentrations below the
 327 drug's S_{eq} , they were found to be thermodynamically stable throughout the course of the study for 8
 328 months, and no CRV precipitation was observed. However, due to the supersaturated concentrations of
 329 CRV in 200%-SNEDDS_{liquid} the potential precipitation during storage is of interest. Therefore, the
 330 200%-SNEDDS_{liquid} were inspected on a regular basis by PLM, and needle-shaped crystals of CRV
 331 were observed after 6 days (see supplementary information, Figure S4).

332 With regards to the stability assessment of the SNEDDS_{FCC}, since PLM could not be employed as a
 333 method to investigate a possible CRV recrystallization during storage from the SNEDDS_{FCC}, the use of
 334 DSC was continued for the physical stability assessment of SNEDDS_{FCC} over a storage period of 10
 335 weeks.

336 The DSC thermograms of 80%-SNEDDS_{FCC} over a storage period of 10 weeks displayed no melting
 337 endotherm for all three solidification ratios (2.5:1, 3.0:1 and 3.5:1 (w/w)) (data not shown). This
 338 confirms that adsorption onto FCC did not cause a loss in the solvent capacity of the SNEDDS_{liquid} over
 339 the storage duration of 10 weeks.

340 The DSC thermograms of 200%-2.5-SNEDDS_{FCC} showed an endothermic event after 3 weeks of
 341 storage with an onset temperature of 110-111 °C corresponding to the onset temperatures of crystalline

342 CRV melting obtained from the thermograms of the PM (Figure 4(A)). In contrast, the SNEDDS_{FCC}
343 with a higher FCC:SNEDDS_{liquid} ratio (200%-3.0-SNEDDS_{FCC} and 200%-3.5-SNEDDS_{FCC}) did not
344 show a melting endotherm even after 10 weeks of storage (Figure 4(B) and Figure 4(C)). It is thus
345 possible that the presence of a higher amount of FCC in the formulation led to a complete incorporation
346 of the 200%-SNEDDS_{liquid} inside the pores of FCC and correspondingly a lower amount of 200%-
347 SNEDDS_{liquid} being present on the FCC surface, thus having an improved stabilizing effect against drug
348 recrystallization, possibly due to spatial confinement of the 200%-SNEDDS_{liquid} in the pores. In
349 summary, comparing the physical stability results from SNEDDS_{FCC} and SNEDDS_{liquid}, it can be
350 concluded that FCC was able to increase the physical stability of the supersaturated concentrations of
351 CRV in the adsorbed SNEDDS_{liquid} when compared to its liquid counterpart (200%-SNEDDS_{liquid}).
352 When comparing the three solidification ratios, the ratio 2.5:1 (w/w), having the lowest amount of FCC,
353 could not retain the supersaturated concentration of CRV in the dissolved state and was found to be
354 stable for only 3 weeks. Thus, the amount of FCC present in the formulation plays a role in stabilizing
355 the supersaturated concentration of CRV against recrystallization.



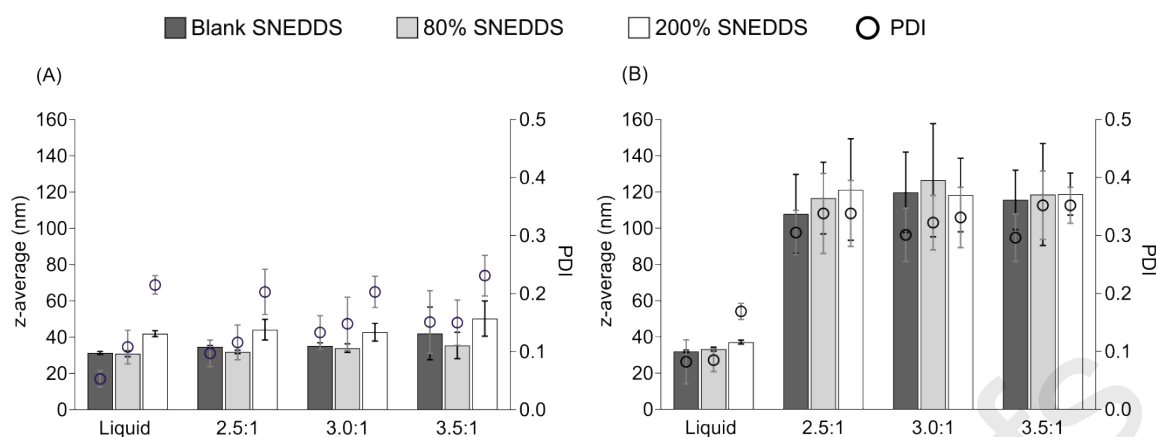
357 **Figure 4.** Enlarged DSC thermograms for the triplicate samples (T1/T2/T3) of (A) 200%-2.5-
358 SNEDDS_{FCC} after 3 weeks; (B) 200%-3.0-SNEDDS_{FCC} after 10 weeks; and (C) 200%-3.5-SNEDDS_{FCC}
359 after 10 weeks of storage under dry conditions at 25 °C. The dashed line with an arrow guides the eye
360 for the melting endotherm of CRV observed in 200%-2.5-SNEDDS_{FCC} and its absence for 200%-3.0-
361 SNEDDS_{FCC} and 200%-3.5-SNEDDS_{FCC}.

362 *Droplet size measurements*

363 Droplet size measurements for SNEDDS_{FCC} were carried out in purified water to assess their ability to
364 form nano-sized emulsions in a comparable way to SNEDDS_{liquid}. Blank-SNEDDS_{liquid} and 80%-
365 SNEDDS_{liquid} emulsified completely after 1 min in purified water forming a translucent dispersion. In
366 contrast, dispersions of 200%-SNEDDS_{liquid} had a slightly bluish appearance, but there were no signs
367 of CRV precipitation after 30 min when investigated by PLM. The droplet size for both blank-
368 SNEDDS_{liquid} and 80%-SNEDDS_{liquid} were found to be around 30 nm, and no statistical difference was
369 observed in the droplet sizes between the blank-SNEDDS_{liquid} and 80%-SNEDDS_{liquid} ($p > 0.05$)
370 demonstrating the formation of nano-sized emulsions (Figure 5 (A)). However, the increased drug load
371 for 200%-SNEDDS_{liquid} resulted in a small but significant increase in droplet size ($p < 0.05$) to 40 nm.
372 This is in agreement with the studies previously performed by Bannow et al. (2020) showing a slight,
373 but significant, increase in the droplet size for drug loadings above the S_{eq} [41].

374 For the SNEDDS_{FCC}, both 80%-SNEDDS_{FCC} and 200%-SNEDDS_{FCC} dispersions had a turbid
375 appearance due to undissolved FCC, hence the dispersions were centrifuged to obtain a clear
376 supernatant prior to DLS analysis. The 80%-SNEDDS_{FCC} and 200%-SNEDDS_{FCC} exhibited a droplet
377 size in the range of 30-35 nm and 40-50 nm, respectively indicating the formation of nano-sized
378 emulsions. Additionally, no statistical difference ($p > 0.05$) in the droplet sizes amongst the three
379 solidification ratios (2.5:1, 3.0:1, and 3.5:1) (w/w) was observed. The PDI for 80%-SNEDDS_{FCC} and
380 200%-SNEDDS_{FCC} was found to be approximately 0.1 and 0.2 respectively, resulting in similar
381 monodisperse systems as observed for the respective SNEDDS_{liquid} (Figure 5 (A)). Overall, the
382 SNEDDS_{liquid} were released from FCC and rapidly dispersed in purified water, demonstrating the ability
383 of SNEDDS_{FCC} to form nano-sized emulsions.

384 To further investigate the effect of the presence of dissolved FCC during the emulsification process on
385 the resulting droplet size and PDI, the dispersion medium was changed from water to HCl solution
386 (0.2M, pH 1.6). All SNEDDS_{liquid} and SNEDDS_{FCC} emulsified completely within 1 min and 5 min
387 respectively and had a translucent appearance. The droplet size for SNEDDS_{liquid} was found to be in the
388 range of 30-40 nm (Figure 5 (B)) similar to the results obtained for the dispersion in purified water.
389 However, for all SNEDDS_{FCC} the presence of dissolved FCC increased the droplet size of the emulsions
390 to 100-120 nm and the PDI to 0.3-0.35. Blank-SNEDDS_{FCC}, 80%-SNEDDS_{FCC} and 200%-SNEDDS_{FCC}
391 thus showed a significant increase ($p < 0.05$) in droplet sizes when compared to their respective liquid
392 counterparts. Additionally, a PDI of 0.3-0.35 indicated the generation of a polydisperse system
393 compared to the monodisperse systems observed under neutral conditions in purified water. However,
394 no statistical difference ($p > 0.05$) in the droplet sizes was observed amongst the three solidification
395 ratios (2.5:1, 3.0:1, and 3.5:1 (w/w)) further confirming no significant impact of the amount of FCC
396 present in the formulations on self-emulsifying properties (in contrast to the above discussed influence
397 on physical stability). However, dispersion of SNEDDS_{FCC} resulted in droplet sizes in the range of 100-
398 120 nm, indicating that the droplet size is still in the nanoemulsion range and solidification with FCC
399 enabled the formation of a nano-sized emulsion.



400

401 **Figure 5:** Droplet size (*columns*) and PDI (*circles*) measured after dispersion of 100 mg of formulation
 402 at 37 °C in 100 mL of (A) Purified water and (B) HCl solution (0.2M, pH 1.6). The data is grouped
 403 according to CRV drug load, starting from SNEDDS_{liquid} to SNEDDS_{FCC} according to the solidification
 404 ratio (2.5:1, 3.0:1, and 3.5:1 (w/w)), from left: blank SNEDDS (*dark grey columns*), center: 80%-
 405 SNEDDS (*light grey columns*) and right: 200%-SNEDDS (*white columns*). Results are represented as
 406 mean ± SD (n=9).

407 *Drug release upon dispersion*

408 As mentioned earlier, incomplete release of drug from formulations containing Neusilin® as the solid
 409 carrier is a concern during the development of solidified LBF [20]. Complete drug release may be
 410 obtained initially in freshly prepared formulations; however, the drug release was found to be reduced
 411 to less than 5% for SEDDS absorbed on neat Neusilin® after 60 days of storage [15].

412 The term ‘dispersion test’ rather than ‘dissolution test’ is used in this study since CRV was released
 413 from FCC along with the SNEDDS_{liquid} and then dispersed in the media as part of a nanoemulsion. The
 414 SNEDDS_{FCC} and their respective SNEDDS_{liquid} were freshly produced before the dispersion studies.

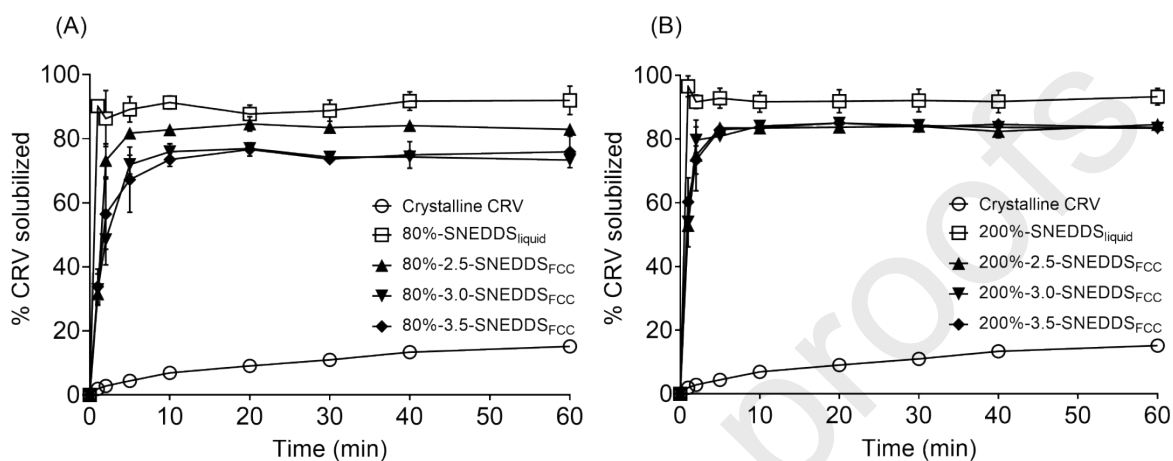
415 A fixed dose of 3.76 mg of CRV was added to the dissolution vessel resulting in varying amounts of
 416 total formulation dosed based on their drug load. The dispersion test was carried out in tap water (pH
 417 7.5) to compare the drug release performance of SNEDDS_{FCC} with their respective SNEDDS_{liquid} and
 418 crystalline CRV. Due to FCC’s poor solubility in tap water (pH 7.5), the employed set-up investigates
 419 the degree of release of the drug-loaded SNEDDS_{liquid} from the FCC carrier. Furthermore, the dispersion
 420 tests were carried out in order to demonstrate the solubility advantage of pre-dissolved CRV in
 421 SNEDDS against the solubility of crystalline CRV at neutral pH, since CRV has a pH-dependent
 422 solubility and shows fast and complete release at acidic pH [42].

423 As shown in Figure 6, crystalline CRV exhibited a slow and incomplete dissolution, resulting in a drug
 424 dissolution of about 15% of the dosed amount of crystalline CRV after 60 min. The SNEDDS_{liquid} and
 425 both SNEDDS_{FCC} with drug loading at their corresponding different solidification ratios (2.5:1, 3.0:1,
 426 and 3.5:1 (w/w)) showed an enhanced rate and extent of drug release compared to crystalline CRV.
 427 Both SNEDDS_{liquid} and SNEDDS_{FCC} demonstrated the same immediate release kinetics, reaching a
 428 plateau of maximum concentration within the first 5 min of the dispersion with no precipitation after
 429 60 min.

430 However, when compared to the respective SNEDDS_{liquid}, the SNEDDS_{FCC} were not able to reach the
 431 same extent of drug release. A possible reason for this could be residual SNEDDS_{liquid} being trapped
 432 inside the pores of FCC and thus not being available during the dispersion process. The total drug
 433 release for 80%-SNEDDS_{liquid} by the end of 60 min was 90%. However, 80%-2.5-SNEDDS_{FCC} showed
 434 a release of 80% in 5 min, while only 70% of drug was released from 80%-3.0-SNEDDS_{FCC} and 80%-

435 3.5-SNEDDS_{FCC} within the same period of time (Figure 6 (A)). These observations suggest that the
 436 amount of FCC present in the formulation plays an important role in governing the drug release
 437 behavior.

438 The 200%-SNEDDS_{liquid} showed a total drug release of 90% after 5 min, which was maintained over
 439 the complete test duration. All 200%-SNEDDS_{FCC} showed a drug release of more than 80% after 5 min
 440 and this level was again maintained for the rest of the study (60 min). No difference in drug release
 441 behavior was observed among the formulations at the three solidification ratios (Figure 6 (B)).

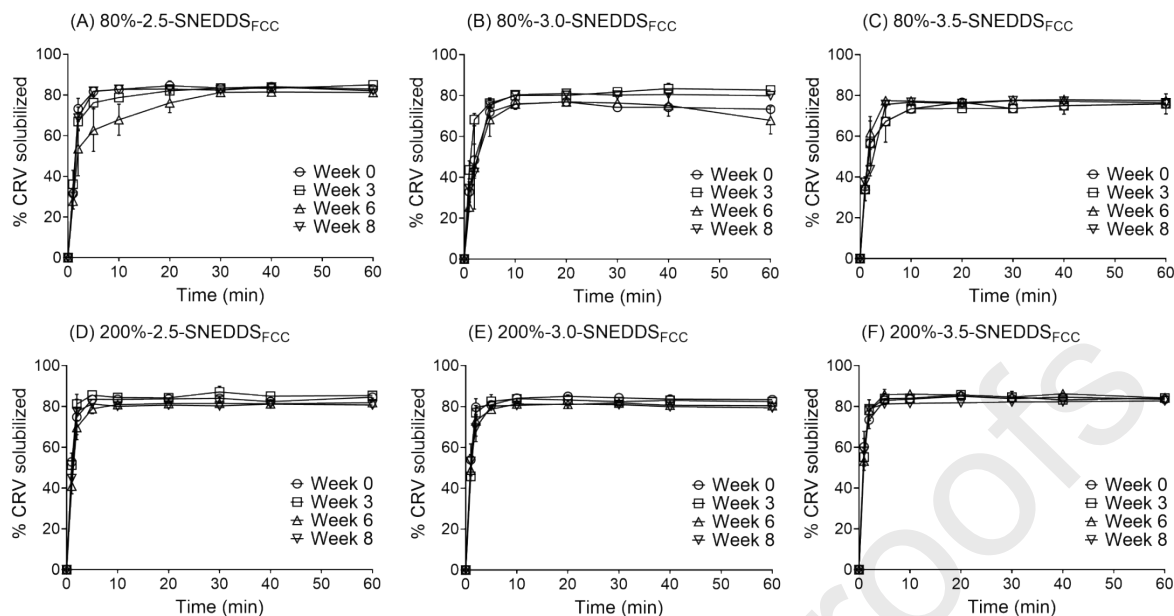


442

443 **Figure 6.** (A) Dispersion profiles of freshly prepared 80%-SNEDDS_{FCC}, 80%-SNEDDS_{liquid} and
 444 dissolution profile of crystalline CRV (all samples dosed at 3.76 mg of CRV). (B) Dispersion profiles
 445 of freshly prepared 200%-SNEDDS_{FCC}, 200%-SNEDDS_{liquid} and dissolution profile of crystalline CRV
 446 (all samples dosed at 3.76 mg of CRV). Tests were carried out in 100 mL tap water (pH 7.5, 37 °C)
 447 stirred at 100 rpm. Results are represented as mean \pm SD (n=3).

448 Figure 7 shows the extent of drug release during 60 min of dispersion testing for 80%-SNEDDS_{FCC} and
 449 200%-SNEDDS_{FCC} after storage under dry conditions at 25 °C for up to 8 weeks, compared to the drug
 450 release observed from freshly prepared samples (week 0). All investigated SNEDDS_{FCC} formulations
 451 showed no significant differences in drug release over a period of 8 weeks of storage ($p > 0.05$). Drug
 452 release from all investigated formulations reached a plateau of maximum concentration within 5 min of
 453 dispersion irrespective of the storage period. Even after 8 weeks of storage, the SNEDDS_{FCC} rapidly
 454 releases the SNEDDS_{liquid} upon contact with the dissolution media and showed spontaneous
 455 emulsification.

456 As discussed above, 200%-2.5-SNEDDS_{FCC} showed an onset of CRV recrystallization after 3 weeks of
 457 storage, which was assumed to influence the *in vitro* drug release behavior. However, the dispersion
 458 profiles indicated no changes in the total amount of CRV released even after 8 weeks of storage. Based
 459 on the LOD of the employed DSC method, the amount of recrystallized CRV after 3 weeks of storage
 460 was estimated to be around 0.08% (w/w) CRV of the total drug amount present (i.e. for
 461 200%-2.5-SNEDDS_{FCC} approximately 0.08% (w/w) of 2.6% (w/w) CRV), which was not sufficient to
 462 have an effect on the resulting *in vitro* drug release performance of the supersaturated SNEDDS_{FCC}.



463

464 **Figure 7.** Dispersion profiles of (A) 80%-2.5-SNEDDS_{FCC}; (B) 80%-3.0-SNEDDS_{FCC}; (C) 80%-3.5-
 465 SNEDDS_{FCC}; (D) 200%-2.5-SNEDDS_{FCC}; (E) 200%-3.0-SNEDDS_{FCC} and (F) 200%-3.5-SNEDDS_{FCC}
 466 of freshly prepared samples (week 0) and after storage under dry conditions at 25 °C for 3, 6 and 8
 467 weeks. The formulations were dosed at 3.76 mg of CRV in 100 mL of tap water (pH 7.5, 37 °C) stirred
 468 at 100 rpm. Results are represented as mean ± SD (n=3).

469 Conclusion

470 In this study, FCC was successfully loaded with conventional SNEDDS_{liquid} and super-SNEDDS_{liquid}
 471 via physical adsorption generating free-flowing powders (SNEDDS_{FCC}) with drug loadings ranging
 472 from 0.8% to 2.6% (w/w) of CRV. FCC stabilized the supersaturated CRV concentrations in the 200%-
 473 3.0-SNEDDS_{FCC} and 200%-3.5-SNEDDS_{FCC} over a storage period of 10 weeks (25 °C at dry
 474 conditions), compared to the observed precipitation of CRV after 6 days of storage in 200%-
 475 SNEDDS_{liquid}. Both the SNEDDS_{FCC} achieved an increased *in vitro* drug release compared to pure
 476 crystalline CRV, however slightly less than their liquid counterparts, indicating that residual
 477 SNEDDS_{liquid} might be trapped in the pores of FCC. FCC as a solid carrier stabilized the supersaturated
 478 solidified SNEDDS and demonstrated the same rate and extent of drug release as freshly prepared
 479 samples even after 8 weeks of storage. The thermodynamic instability of supersaturated LBF, resulting
 480 in the precipitation of drug during storage, has hindered a more widespread application of super-
 481 SNEDDS_{liquid} in the field of oral drug delivery. However, the results of the current study indicate that
 482 loading super-SNEDDS_{liquid} on FCC can greatly improve their physical stability.

483 References

- 484 [1] M.S. Alqahtani, M. Kazi, M.A. Alsenaidy, M.Z. Ahmad, *Advances in Oral Drug Delivery*,
 485 *Front. Pharmacol.* 12 (2021) 62. <https://doi.org/10.3389/fphar.2021.618411>.
- 486 [2] J. Huang, *Formulation Forum: Amorphous Nanoparticles for Drug Delivery of Poorly Water-*
 487 *Soluble Compounds*, *Drug Dev. Deliv.* 21 (2021) 16–19. [https://doi.org/drug-](https://doi.org/drug-dev.com/formulation-forum-amorphous-nanoparticles-for-drug-delivery-of-poorly-water-soluble-compound)
 488 [dev.com/formulation-forum-amorphous-nanoparticles-for-drug-delivery-of-poorly-water-](https://doi.org/drug-dev.com/formulation-forum-amorphous-nanoparticles-for-drug-delivery-of-poorly-water-soluble-compound)
 489 [soluble-compound](https://doi.org/drug-dev.com/formulation-forum-amorphous-nanoparticles-for-drug-delivery-of-poorly-water-soluble-compound).
- 490 [3] T. Loftsson, M.E. Brewster, *Pharmaceutical applications of cyclodextrins: Basic science and*
 491 *product development*, *J. Pharm. Pharmacol.* 62 (2010) 1607–1621.
 492 <https://doi.org/10.1111/j.2042-7158.2010.01030.x>.

- 493 [4] S.T. Buckley, K.J. Frank, G. Fricker, M. Brandl, Biopharmaceutical classification of poorly
494 soluble drugs with respect to “enabling formulations,” *Eur. J. Pharm. Sci.* 50 (2013) 8–16.
495 <https://doi.org/10.1016/j.ejps.2013.04.002>.
- 496 [5] C.W. Pouton, Lipid formulations for oral administration of drugs: Non-emulsifying, self-
497 emulsifying and “self-microemulsifying” drug delivery systems, *Eur. J. Pharm. Sci.* 11 (2000)
498 93–98. [https://doi.org/10.1016/S0928-0987\(00\)00167-6](https://doi.org/10.1016/S0928-0987(00)00167-6).
- 499 [6] C.W. Pouton, Formulation of poorly water-soluble drugs for oral administration:
500 Physicochemical and physiological issues and the lipid formulation classification system, *Eur.*
501 *J. Pharm. Sci.* 29 (2006) 278–287. <https://doi.org/10.1016/j.ejps.2006.04.016>.
- 502 [7] N. Thomas, T. Rades, A. Müllertz, Recent developments in oral lipid-based drug delivery, *J.*
503 *Drug Deliv. Sci. Technol.* 23 (2013) 375–382. [https://doi.org/10.1016/S1773-2247\(13\)50054-](https://doi.org/10.1016/S1773-2247(13)50054-2)
504 2.
- 505 [8] R.N. Gursoy, S. Benita, Self-emulsifying drug delivery systems (SEDDS) for improved oral
506 delivery of lipophilic drugs, *Biomed. Pharmacother.* 58 (2004) 173–182.
507 <https://doi.org/10.1016/j.biopha.2004.02.001>.
- 508 [9] N. Thomas, R. Holm, A. Müllertz, T. Rades, In vitro and in vivo performance of novel
509 supersaturated self-nanoemulsifying drug delivery systems (super-SNEDDS), *J. Control.*
510 *Release.* 160 (2012) 25–32. <https://doi.org/10.1016/j.jconrel.2012.02.027>.
- 511 [10] H. Park, E.S. Ha, M.S. Kim, Current status of supersaturable self-emulsifying drug delivery
512 systems, *Pharmaceutics.* 12 (2020). <https://doi.org/10.3390/pharmaceutics12040365>.
- 513 [11] N. Thomas, R. Holm, M. Garmer, J.J. Karlsson, A. Müllertz, T. Rades, Supersaturated self-
514 nanoemulsifying drug delivery systems (Super-SNEDDS) enhance the bioavailability of the
515 poorly water-soluble drug simvastatin in dogs, *AAPS J.* 15 (2013) 219–227.
516 <https://doi.org/10.1208/s12248-012-9433-7>.
- 517 [12] H.B. Schultz, N. Thomas, S. Rao, C.A. Prestidge, Supersaturated silica-lipid hybrids (super-
518 SLH): An improved solid-state lipid-based oral drug delivery system with enhanced drug
519 loading, *Eur. J. Pharm. Biopharm.* 125 (2018) 13–20.
520 <https://doi.org/10.1016/j.ejpb.2017.12.012>.
- 521 [13] S. Inugala, B.B. Eedara, S. Sunkavalli, R. Dhurke, P. Kandadi, R. Jukanti, S. Bandari, Solid
522 self-nanoemulsifying drug delivery system (S-SNEDDS) of darunavir for improved
523 dissolution and oral bioavailability: In vitro and in vivo evaluation, *Eur. J. Pharm. Sci.* 74
524 (2015) 1–10. <https://doi.org/10.1016/j.ejps.2015.03.024>.
- 525 [14] M. Van Speybroeck, H.D. Williams, T.H. Nguyen, M.U. Anby, C.J.H. Porter, P. Augustijns,
526 Incomplete desorption of liquid excipients reduces the in vitro and in vivo performance of self-
527 emulsifying drug delivery systems solidified by adsorption onto an inorganic mesoporous
528 carrier, *Mol. Pharm.* 9 (2012) 2750–2760. <https://doi.org/10.1021/mp300298z>.
- 529 [15] S.G. Gumaste, B.O.S. Freire, A.T.M. Serajuddin, Development of solid SEDDS, VI: Effect of
530 precoating of Neusilin® US2 with PVP on drug release from adsorbed self-emulsifying lipid-
531 based formulations, *Eur. J. Pharm. Sci.* 110 (2017) 124–133.
532 <https://doi.org/10.1016/j.ejps.2017.02.022>.
- 533 [16] P. Joyce, T.J. Dening, T.R. Meola, H.B. Schultz, R. Holm, N. Thomas, C.A. Prestidge,
534 Solidification to improve the biopharmaceutical performance of SEDDS: Opportunities and
535 challenges, *Adv. Drug Deliv. Rev.* 142 (2019) 102–117.

- 536 <https://doi.org/10.1016/j.addr.2018.11.006>.
- 537 [17] T.J. Dening, S. Rao, N. Thomas, C.A. Prestidge, Novel Nanostructured Solid Materials for
538 Modulating Oral Drug Delivery from Solid-State Lipid-Based Drug Delivery Systems, *AAPS*
539 *J.* 18 (2016) 23–40. <https://doi.org/10.1208/s12248-015-9824-7>.
- 540 [18] J. Mandić, A. Zvonar Pobirk, F. Vrečer, M. Gašperlin, Overview of solidification techniques
541 for self-emulsifying drug delivery systems from industrial perspective, *Int. J. Pharm.* 533
542 (2017) 335–345. <https://doi.org/10.1016/j.ijpharm.2017.05.036>.
- 543 [19] C. Alvebratt, T.J. Dening, M. Åhlén, O. Cheung, M. Strømme, A. Gogoll, C.A. Prestidge,
544 C.A.S. Bergström, In vitro performance and chemical stability of lipid-based formulations
545 encapsulated in a mesoporous magnesium carbonate carrier, *Pharmaceutics*. 12 (2020) 1–15.
546 <https://doi.org/10.3390/pharmaceutics12050426>.
- 547 [20] H.D. Williams, M. Van Speybroeck, P. Augustijns, C.J.H. Porter, Lipid-based formulations
548 solidified via adsorption onto the mesoporous carrier neusilin® US2: Effect of drug type and
549 formulation composition on in vitro pharmaceutical performance, *J. Pharm. Sci.* 103 (2014)
550 1734–1746. <https://doi.org/10.1002/jps.23970>.
- 551 [21] S.G. Gumaste, S.A. Pawlak, D.M. Dalrymple, C.J. Nider, L.D. Trombetta, A.T.M. Serajuddin,
552 Development of Solid SEDDS, IV: Effect of Adsorbed Lipid and Surfactant on Tableting
553 Properties and Surface Structures of Different Silicates, *Pharm. Res.* 30 (2013) 3170–3185.
554 <https://doi.org/10.1007/s11095-013-1114-4>.
- 555 [22] A. Tan, S. Rao, C.A. Prestidge, Transforming lipid-based oral drug delivery systems into solid
556 dosage forms: An overview of solid carriers, physicochemical properties, and
557 biopharmaceutical performance, *Pharm. Res.* 30 (2013) 2993–3017.
558 <https://doi.org/10.1007/s11095-013-1107-3>.
- 559 [23] S. Beg, S. Swain, H.P. Singh, C.N. Patra, M.E.B. Rao, Development, Optimization, and
560 Characterization of Solid Self-Nanoemulsifying Drug Delivery Systems of Valsartan Using
561 Porous Carriers, *AAPS PharmSciTech.* 13 (2012) 1416–1427. <https://doi.org/10.1208/s12249-012-9865-5>.
- 563 [24] S. Beg, O.P. Katare, S. Saini, B. Garg, R.K. Khurana, B. Singh, Solid self-nanoemulsifying
564 systems of olmesartan medoxomil: Formulation development, micromeritic characterization,
565 in vitro and in vivo evaluation, *Powder Technol.* 294 (2016) 93–104.
566 <https://doi.org/10.1016/j.powtec.2016.02.023>.
- 567 [25] Y. Ito, H. Arai, K. Uchino, K. Iwasaki, N. Shibata, K. Takada, Effect of adsorbents on the
568 absorption of lansoprazole with surfactant, *Int. J. Pharm.* 289 (2005) 69–77.
569 <https://doi.org/10.1016/j.ijpharm.2004.10.010>.
- 570 [26] A. Deshmukh, S. Kulkarni, Solid self-microemulsifying drug delivery system of ritonavir,
571 *Drug Dev. Ind. Pharm.* 40 (2014) 477–487. <https://doi.org/10.3109/03639045.2013.768632>.
- 572 [27] M. Milović, J. Djuriš, L. Djekić, D. Vasiljević, S. Ibrić, Characterization and evaluation of
573 solid self-microemulsifying drug delivery systems with porous carriers as systems for
574 improved carbamazepine release, *Int. J. Pharm.* 436 (2012) 58–65.
575 <https://doi.org/10.1016/j.ijpharm.2012.06.032>.
- 576 [28] V. Agarwal, A. Siddiqui, H. Ali, S. Nazzal, Dissolution and powder flow characterization of
577 solid self-emulsified drug delivery system (SEDDS), *Int. J. Pharm.* 366 (2009) 44–52.
578 <https://doi.org/10.1016/j.ijpharm.2008.08.046>.

- 579 [29] J.H. Kang, D.H. Oh, Y.K. Oh, C.S. Yong, H.G. Choi, Effects of solid carriers on the
580 crystalline properties, dissolution and bioavailability of flurbiprofen in solid self-
581 nanoemulsifying drug delivery system (solid SNEDDS), in: *Eur. J. Pharm. Biopharm.*,
582 Elsevier, 2012: pp. 289–297. <https://doi.org/10.1016/j.ejpb.2011.11.005>.
- 583 [30] S.G. Gumaste, D.M. Dalrymple, A.T.M. Serajuddin, Development of solid SEDDS, V:
584 Compaction and drug release properties of tablets prepared by adsorbing lipid-based
585 formulations onto neusilin® US2, *Pharm. Res.* 30 (2013) 3186–3199.
586 <https://doi.org/10.1007/s11095-013-1106-4>.
- 587 [31] R.N. Dash, H. Mohammed, T. Humaira, A.V. Reddy, Solid supersaturatable self-
588 nanoemulsifying drug delivery systems for improved dissolution, absorption and
589 pharmacodynamic effects of glipizide, *J. Drug Deliv. Sci. Technol.* 28 (2015) 28–36.
590 <https://doi.org/10.1016/j.jddst.2015.05.004>
- 591 [32] D. Preisig, D. Haid, F.J.O. Varum, R. Bravo, R. Alles, J. Huwyler, M. Puchkov, Drug loading
592 into porous calcium carbonate microparticles by solvent evaporation, *Eur. J. Pharm. Biopharm.*
593 87 (2014) 548–558. <https://doi.org/10.1016/j.ejpb.2014.02.009>.
- 594 [33] T. Stirnimann, S. Atria, J. Schoelkopf, P.A.C. Gane, R. Alles, J. Huwyler, M. Puchkov,
595 Compaction of functionalized calcium carbonate, a porous and crystalline microparticulate
596 material with a lamellar surface, *Int. J. Pharm.* 466 (2014) 266–275.
597 <https://doi.org/10.1016/j.ijpharm.2014.03.027>.
- 598 [34] T. Stirnimann, N. Di Maiuta, D.E. Gerard, R. Alles, J. Huwyler, M. Puchkov, Functionalized
599 calcium carbonate as a novel pharmaceutical excipient for the preparation of orally dispersible
600 tablets, *Pharm. Res.* 30 (2013) 1915–1925. <https://doi.org/10.1007/s11095-013-1034-3>.
- 601 [35] D. Preisig, R. Roth, S. Tognola, F.J.O. Varum, R. Bravo, Y. Cetinkaya, J. Huwyler, M.
602 Puchkov, Mucoadhesive microparticles for local treatment of gastrointestinal diseases, *Eur. J.*
603 *Pharm. Biopharm.* 105 (2016) 156–165. <https://doi.org/10.1016/j.ejpb.2016.06.009>.
- 604 [36] R. Roth, J. Schoelkopf, J. Huwyler, M. Puchkov, Functionalized calcium carbonate
605 microparticles for the delivery of proteins, *Eur. J. Pharm. Biopharm.* 122 (2018) 96–103.
606 <https://doi.org/10.1016/j.ejpb.2017.10.012>.
- 607 [37] L. Wagner-Hattler, K. Wyss, J. Schoelkopf, J. Huwyler, M. Puchkov, In vitro characterization
608 and mouthfeel study of functionalized calcium carbonate in orally disintegrating tablets, *Int. J.*
609 *Pharm.* 534 (2017) 50–59. <https://doi.org/10.1016/j.ijpharm.2017.10.009>.
- 610 [38] V.A. Eberle, J. Schoelkopf, P.A.C. Gane, R. Alles, J. Huwyler, M. Puchkov, Floating
611 gastroretentive drug delivery systems: Comparison of experimental and simulated dissolution
612 profiles and floatation behavior, *Eur. J. Pharm. Sci.* 58 (2014) 34–43.
613 <https://doi.org/10.1016/j.ejps.2014.03.001>.
- 614 [39] J. Liu, T. Rades, I. Tho, E.O. Kissi, Functionalised calcium carbonate as a cofomer to
615 stabilize amorphous drugs by mechanochemical activation, *Eur. J. Pharm. Biopharm.* 155
616 (2020) 22–28. <https://doi.org/10.1016/j.ejpb.2020.07.029>.
- 617 [40] J. Bannow, L. Koren, S. Salar-Behzadi, K. Löbmann, A. Zimmer, T. Rades, Hot melt coating
618 of amorphous carvedilol, *Pharmaceutics.* 12 (2020) 1–13.
619 <https://doi.org/10.3390/pharmaceutics12060519>.
- 620 [41] J. Bannow, Y. Yorulmaz, K. Löbmann, A. Müllertz, T. Rades, Improving the drug load and in
621 vitro performance of supersaturated self-nanoemulsifying drug delivery systems (super-

- 622 SNEDDS) using polymeric precipitation inhibitors, *Int. J. Pharm.* 575 (2020) 118960.
623 <https://doi.org/10.1016/j.ijpharm.2019.118960>.
- 624 [42] R. Hamed, A. Awadallah, S. Sunoqrot, O. Tarawneh, S. Nazzal, T. AlBaraghthi, J. Al Sayyad,
625 A. Abbas, pH-Dependent Solubility and Dissolution Behavior of Carvedilol—Case Example
626 of a Weakly Basic BCS Class II Drug, *AAPS PharmSciTech.* 17 (2016) 418–426.
627 <https://doi.org/10.1208/s12249-015-0365-2>.

Journal Pre-proofs